交通部中央氣象局委託研究計畫報告

WRF 模式降水預報之改進與研究

計畫類別：□國內 ■國外

計畫編號：MOTC-CWB-98- 3M-04

執行期間：98 年 2 月 26 日至 98 年 12 月 31 日

計畫主持人： 陶為國

執行單位：
Lanshing Hwang Landscape Architecture, Planning and Urban Design

中華民國 98 年 12 月

98 年度政府部門科技計畫期末摘要報告

計畫名稱 Studying the precipitation forecast and simulation with improved WRF

審議編號：	x	部會署原計畫編號：	MOTC-CWB-98- 3M-04
主管機關：	交通部中央氣象局	執行單位：	*Lanshing Hwang Landscape Architecture, Planning and Urban Design*
計畫主持人：	陶為國	聯絡人：	Lanshing Hwang
電話號碼：	301-552-1173	傳真號碼：	301-552-1173
期程：	98 年 2 月 26 日至 98 年 12 月 31 日		
經費：（全程）	790 仟元	經費(年度)	790 仟元

執行情形：

1.執行進度：

	預定（%）	實際（%）	比較（%）
當年	100	100	0
全程	100	100	0

2.經費支用：

	預定	實際	支用率（%）
當年	100	100	
全程	100	100	

3.主要執行成果：

1) Implemented a new radiation scheme into CWB WRF (V3.1)
2) Provided an off-line convective – stratifiorm separation scheme to CWB
3) Conducted high-resolution WRF simulations for two convective systems during SoWMEX/TiMREX 2008
4) Provided an improved evaporation of rain (based on result from spectral bin microphysical scheme)
5) Provided an improved microphysical scheme that reduced un-realistic high 40 dBZ at high altitude
6) Conducted high-resolution WRF simulation for Typhoon Morakot 2009.

4.計畫變更說明： None

5.落後原因： None

6.主管機關之因應對策（檢討與建議）：

Studying the precipitation forecast and simulation with improved WRF

MOTC-CWB-98-3M-04

Final Report

Wei-Kuo Tao
Lanshing Hwang Landscape Architecture, Planning and Urban Design
9008 Brae Brook Drive
Lanham, Maryland
USA, 20706

Mei-Yu Chang
Central Weather Bureau
64 Kung Yuan Road
Taipei, Taiwan
Republic of China

November 30 2009

Summary

Advances in computing power allow atmospheric prediction models to be run at progressively finer scales of resolution, using increasingly more sophisticated physical parameterizations and numerical methods. The representation of cloud microphysical processes is a key component of these models, over the past decade both research and operational numerical weather prediction models [i.e., the Fifth-generation National Center for Atmospheric Research (NCAR)/Penn State University Mesoscale Model (MM5), the National Centers for Environmental Prediction (NCEP) Eta, and the Weather Research and Forecasting Model (WRF)] have started using more complex microphysical schemes that were originally developed for high-resolution cloud-resolving models (CRMs). CRMs, which are run at horizontal resolutions on the order of 1-2 km or finer, can simulate explicitly complex dynamical and microphysical processes associated with deep, precipitating atmospheric convection. A recent report to the United States Weather Research Program (USWRP) Science Steering Committee specifically calls for the replacement of implicit cumulus parameterization schemes with explicit bulk schemes in numerical weather prediction (NWP) as part of a community effort to improve quantitative precipitation forecasts (QPF).

A sophisticated cloud microphysics parameterization has been implemented into a high-resolution non-hydrostatic weather research and forecast system (WRF). This cloud microphysics scheme has been extensively tested and applied for various clouds/cloud systems in different geographic locations. It includes a parameterized two-category liquid water scheme (cloud water and rain), and a parameterized three-category ice scheme (cloud ice, snow and hail/graupel). The snow, hail/graupel and rain are heavier particles that fall relative to the cloud updraft with appreciable terminal velocities. These precipitation particles (rain, snow and graupel/hail) ultimately fall to the ground as rainfall and/or snowfall that is one of the most important factors for determining the QPF.

The cloud microphysics parameterization on precipitation and rainfall in the WRF needs to be investigated. Specifically, we have (1) continued improving, testing and evaluating the performance of the microphysical scheme for heavy precipitation events, (2) conducted both case study (Typhoon Marokot) and real time forecast to evaluate the performance of the CWB's WRF, and (3) examined the sensitivity of model resolution on precipitation processes and surface rainfall amount. In addition, we implemented improved radiation schemes (both long- and short-wave radiative transfer) in CWB/s WRF. We also provided software on separating convective and stratiform rain.

It is expected that these WRF modeling research at CWB can provide precipitation and rainfall forecast and related information to the operational unit for reference and guidance.

1. Introduction

Recent significant increases in computer power allow Numerical Weather Prediction (NWP) to be run at fine grid sizes. NWP can therefore include the more sophisticated microphysical processes that have been developed for Cloud Resolving Models (CRMs) over the past few decades. A recent report to the United States Weather Research Program (USWRP) Science Steering Committee specifically calls for the replacement of implicit cumulus parameterization schemes with explicit bulk schemes as part of a community effort to improve the model Quantitative Precipitation Forecasts (QPF) (Fritsch and Carbone 2002). Consequently, NWP should be able to improve its QPF. Such a move cannot, however, be expected to improve the QPF unless the forecast initializations of precipitation are at least in reasonable agreement with observations.

However, traditional convective parameterization (i.e., Kain-Fritsch, Betts-Miller-Janjic, Arakawa and Schubert and others) is still needed for NWP and global models for long-term forecasts. Many convective parameterization schemes and processes may be grid size and case dependent (Rogers and Fritsch 1996; Wang and Seaman 1997; Gallus 1999; Yang and Tung 2003 and others). Also, it was recognized that no parameterization scheme is designed for a 10-20 km grid (Tao *et al.* 2003b). Molinari and Dudek (1992) suggested that a "hybrid scheme" in which a cumulus parameterization and an explicit moisture scheme interact directly and simultaneously, could be a possible solution. The cumulus parameterization scheme is generally used to represent convective precipitation and the explicit moisture scheme to represent grid-resolvable precipitation such as stratiform/anvil rain. How to allow the direct interaction between the two processes is a very difficult issue and needs future investigations.

There is no doubt that cloud microphysics play an important role in non-hydrostatic high-resolution simulations as evidenced by the extensive amount of research devoted to the development and improvement of cloud microphysical schemes and their application to the study of precipitation processes, hurricanes and other severe weather events over the past two and a half decades (see Table 1). Many different approaches have been used to examine the impact of microphysics on precipitation processes associated with convective systems[1]. For example, new ice phase schemes were developed in the 80's (Lin *et al.* 1983; Cotton *et al.* 1982, 1986; Rutledge and Hobbs 1984), and the impact of those ice processes on precipitation processes associated with deep convection were investigated (Yoshizaki 1986; Nicholls 1987; Fovell and Ogura 1988; Tao and Simpson 1989; and others). The results suggested that the propagation speed and cold outflow structure were similar between runs with and without ice-phase processes. This is because evaporative cooling and the vertical shear of the horizontal wind in the lower troposphere largely determine the outflow structure. However, ice phase microphysical processes are crucial for developing a realistic stratiform structure and precipitation statistics. The sensitivity of the different types of microphysical schemes and processes on precipitation was also investigated (i.e., McCumber *et al.* 1991; Ferrier *et al.* 1995; Wu *et al.* 1999; Tao *et al. 2003a;* and others). Those results indicated that the use of three ice classes produces better results than two classes ice, and for tropical cumuli, the optimal mix of bulk ice hydrometeors is cloud-ice, snow and graupel (i.e., McCumber *et al.* 1991). Ice microphysical processes also play an important role in the long-term simulation of cloud properties and cloud-radiative properties (i.e., Wu *et al.* 1999; Zeng *et al.* 2008). Additionally, water budgets and process diagrams (see Fig. 7 in Tao *et al.* 1991 and Fig. 10 in Colle and Zeng 2004) were analyzed to determine the dominant cloud and precipitation processes (i.e., Fovell and Ogura 1988; Tao *et al.* 1991; Colle and Zeng 2004; and Colle *et al.* 2005). For example, Fovell and Ogura (1988) found that

[1] The effects of aerosols (see a brief review by Tao *et al.* 2007) on microphysical (processes) schemes have also been studied.

the melting of hail was the primary source of rain for a long lasting mid-latitude squall line. Tao *et al.* (1991) showed that the dominant microphysical processes were quite different between the convective and stratiform regions and between the mature and decaying stages. Condensation, collection (accretion) of cloud water by rain, and melting of graupel dominated in the convective region, while deposition, evaporation, melting and accretion associated with the ice phase dominated during the mature phase of a tropical squall line. However, melting and sublimation became important during the dissipating stage in the stratiform region. Colle *et al.* (2005) determined that condensation, snow deposition, accretion of cloud water by rain and melting are important processes associated with orographic precipitation events.

Many new and better microphysical parameterization schemes were also developed in the past decade (i.e., Ferrier 1994; Meyers *et al.* 1997; Resiner *et al.* 1998; Hung *et al.* 2004; Walko *et al.* 2005; Morrison *et al.* 2005a,b; Straka and Mansell 2005; Milbrandt and Yau 2005; Morrison and Grabowski, 2008; Thompson *et al.* 2004, 2008; Dudhia *et al.* 2008 and others). These schemes range from one-moment bulk with three ice classes to one-moment bulk with multiple ice classes to two-moment two, three and four classes of ice. However, only idealized simulations have been conducted to test new microphysical schemes. In addition, some of modeling research has only been performed to examine specific microphysical processes (i.e., turning melting/evaporation on or off, reducing the auto-conversion rate from cloud water to rain, etc.) within one particular microphysical scheme (i.e., evaporation, melting of large precipitating ice particles, etc.) responsible for determining the organization and structure of convective systems (i.e., Tao *et al.* 1995; Wang 2002; Colle *et al.* 2005; Zhu and Zhang 2006; and many others).

The proposed research will focus on both real case studies and operational modes to examine the performance of the Goddard microphysical scheme. The Goddard scheme includes a parameterized two-category liquid water scheme (cloud water and rain), and a parameterized three-category ice scheme (cloud ice, snow and hail/graupel). The snow, hail/graupel and rain are heavier particles that fall relative to the cloud updraft with appreciable terminal velocities. These precipitation particles (rain, snow and graupel/hail) ultimately fall to the ground as rainfall and/or snowfall that is one of the most important factors for determining the QPF. The major objective of this one-year proposed research is to continue improving and evaluating the performance of this microphysics in WRF. The sensitivity tests will be also conducted to investigate the impact of the grid sizes on the microphysical parameterization and its predicted strength and evolution of rainfall. Numerical experiments will be also performed for selected severe weather events over the Taiwan area. This proposed research could advance both the QPF and regional climate modeling research through better understanding of cloud and precipitation processes and their interaction with radiation and surface processes. It is also recognized that comparison studies with observational data (i.e., from radar and rain gauge) collected over the Taiwan region are needed to validate the cloud microphysics schemes.

	Model	*Microphysics*	*Resolutions Vertical Layers*	*Integration Time*	*Case*
Lin *et al.* (1983)	2D	3-ICE	200 m/95	48 min	Hail Event Montana
Cotton *et al.* (1982, 1986)	2D	3-ICE & Ni	500 m/31	5 hours	Orographic Snow
Rutledge and Hobbs (1984)	2D Kinematics	3-ICE	600 m/20	Steady State	Narrow Cold Front
Lord *et al.* (1984)	2D axisymmetric	3-ICE vs Warm Rain	2 km/20	4.5 days	Idealized
Yoshizaki (1986)#	2D slab-symmetric	3-ICE scheme vs Warm Rain	0.5 km/32	4.5 hours	12 September GATE Squall Line
Nicholls (1987)	2D slab-symmetric	3-ICE vs Warm Rain	0.5 km/25	5 hours	12 September GATE Squall Line
Fovell and Ogura (1988)	2D slab-symmetric	3-ICE vs Warm Rain	1 km/31	10 hours	Mid-latitude Squall Line
Tao and Simpson (1989, 1993)	2D and 3D	3-ICE vs Warm Rain	1 km/31	12 hours	GATE Squall Line
Tao *et al.* (1990)	2D	3-ICE	1 km/31	12 hours	GATE Squall Line
McCumber *et al.* (1991)	2D and 3D	3-ICE scheme (graupel vs hail, 2ICE vs 3ICE)	1 km/31	12 hours	GATE Squall Line
Wu *et al.* (1999)	2D slab-symmetric	2 ICE	3 km/52	39 days	TOGA COARE
Ferrier (1994), Ferrier *et al.* (1995)	2D slab-symmetric	2-moment 4-ICE	1 km/31	12 hours	COHMEX, GATE Squall Line
Tao *et al.* (1995)	2D slab-symmetric	3-ICE	0.75 and 1 km/31	12 hours	EMEX, PRESTORM
Walko *et al.* (1995)	2D	4-ICE	0.3 km/80	30 min	Idealized
Meyers *et al.* (1997)	2D	2-moment 4-ICE	0.5 km/80	30 min	Idealized
Straka and Mansell (2005)	3D	10-ICE	0.5 km/30?	~2 hours	Idealized
Lang *et al.* (2007)	3D	3-ICE	.25 to 1km /41	8 hours	LBA
Zeng *et al.* (2008)	2D and 3D	3-ICE	1 km/41	40 days	SCSMEX, KWAJEX
Milbrandt and Yau (2005)	1D	Three-moment	/51	50 minutes	Idealized Hail Storm
Morrison *et al.* (2005)	Single column model	Two moments and 2-ICE	Single column model 27 layers	3 days	SHEBA FIRE-FACE
Morrison and Grabowski (2008)	2D	Two-moment ICE	50 m/60	90 minutes	Idealized
Reisner *et al.* (1998)	MM5 Non-hydrostatic	3-ICE and 2-moment for ICE	2.2 km/27	6 hours (2.2 km grid)	Winter Storms
Thompson *et al.* (2004)	MM5 2D	3-ICE	10 km/39	3 hours	Idealized
Thompson *et al.* (2008)	WRF 2D	3-ICE	10 km/39	6 hours	Idealized
Colle and Mass (2000)	MM5 Non-hydrostatic	3-ICE	1.33 km/38	96 hours	Orographic Flooding
Colle and Zeng (204)	2-D MM5 Non-hydrostatic	3-ICE	1.33 km/39	12 hours	Orographic
Colle *et al.* (2005)	MM5 Non-hydrostatic	3-ICE	1.33 km/320	36 hours	IMPROVE
Yang and Ching (2005)	MM5 Non-hydrostatic	3-ICE	6.67 km/23	2.5 days	Typhoon Toraji (2001)
Zhu and Zhang (2006)	MM5 Non-hydrostatic	3-ICE	4 km/24	5 days	Bonnie (1998)
Wang (2002)	TCM3-hydrostatic	3-ICE	5 km/21	5 days	Idealized
Hong *et al.* (2004)	WRF Non-hydrostatic	3-ICE	45 km/23	48 hours	Korean Heavy Rainfall event
Li and Pu (2008)	WRF Non-hydrostatic	2-ICE and 3-ICE	3 km/31	1.25 days	Hurricane Emily (2005)
Jankov *et al.* (2005; 2007)	WRF Non-hydrostatic	2-ICE and 3ICE	12 km/31	1 day	IHOP
Dudhia *et al.* (2008)	WRF Non-hydrostatic	3-ICE	5 km/31	1.5 days	Korean Heavy Snow event
Tao *et al.* (2010)	WRF Non-hydrostatic	2-ICE, 3ICE and warm rain	1.667 km/31	3 days	Hurricane Katrina (2005)

Table 1 Key papers using high-resolution numerical cloud models (including those that developed new improved microphysical schemes) to study the impact of microphysical schemes on precipitation. Model type (2D or 3D), microphysical scheme (one moment or multi-moment bulk), resolution (km), number of vertical layers, time step (seconds), case and integration time (hours) are all listed.. TCM3 stands for the "Tropical Cyclone Model with triple nested movable mesh". Also only papers with bulk schemes are listed. MM5 stands for the Penn State/NCAR Mesoscale Model Version 5.

2. Methodology

The WRF is a next-generation mesoscale forecast model and assimilation system that will be used to advance the understanding and the prediction of mesoscale precipitation systems. The model will incorporate advanced dynamics, numeric and data assimilation techniques, a multiple re-locatable nesting capability, and improved physical packages. The WRF model will be used for a wide range of applications, from idealized research to operational forecasting, with an emphasis on horizontal grid sizes in the range of 1-10 km. The WRF will be a candidate to replace existing research and forecast models (i.e., MM5, NCEP/ETA).

At Goddard, the modeling and dynamic group has implement several ice schemes (Tao *et al.* 2003a; Lang *et al.* 2007 and Zeng *et al.* 2008) into WRF V2.2, V2.2.1 and V3.1. The Goddard radiation (including explicitly calculated cloud optical properties) is recently implementing into and testing into WRF3.1. WRF can also be initialized with the Goddard Earth Observing System (GEOS) global analyses. This link between the GEOS global analyses and the WRF models could allow for many useful regional modeling applications. For example, a series of weeklong WRF simulations were conducted to test the sensitivity of the initial and boundary conditions derived from NCEP, ECMWF, and GEOS on simulations of precipitation and chemistry (for air pollution study) transport over the eastern USA and East Asia

The Goddard Cumulus Ensemble (GCE) model's (Tao and Simpson 1993) one-moment bulk microphysical schemes were implemented into WRF. These schemes are mainly based on Lin *et al.* (1983) with additional processes from Rutledge and Hobbs (1984). However, the Goddard microphysics schemes have several modifications. First, there is an option to choose either graupel or hail as the third class of ice (McCumber *et al.* 1991). Graupel has a relatively low density and a high intercept value (i.e., more numerous small particles). In contrast, hail has a relative high density and a low intercept value (i.e., more numerous large particles). These differences can affect not only the description of the hydrometeor population and formation of the anvil-stratiform region but also the relative importance of the microphysical-dynamical-radiative processes. Second, a new saturation technique (Tao *et al.* 1989) was added. This saturation technique is basically designed to ensure that super saturation (sub-saturation) cannot exist at a grid point that is clear (cloudy). The saturation scheme is one of the last microphysical processes to be computed. It is only done prior to evaluating evaporation of rain and deposition or sublimation of snow/graupel/hail. Third, all microphysical processes that do not involve melting, evaporation or sublimation (i.e., transfer rates from one type of hydrometeor to another) are calculated based on one thermodynamic state. This ensures that all of these processes are treated equally. The opposite approach is to have one particular process calculated first modifying the temperature and water vapor content (i.e., through latent heat release) before the next process is computed. Fourth, the sum of all sink processes associated with one species will not exceed its mass. This ensures that the water budget will be balanced in the microphysical calculations[2].

In addition to the two different 3ICE schemes (i.e., cloud ice, snow and graupel or cloud ice, snow and hail) implemented into WRF 2.2.1 and 3.1, the Goddard microphysics has other two options. The first one is equivalent to a two-ice (2ICE) scheme having only cloud ice and snow. This option may be needed for coarse resolution simulations (i.e., > 5 km grid size). The two-class ice scheme could be applied for winter and frontal convection (Tao *et al.* 2009; Shi *et al.* 2009). The second one is a warm rain only (cloud water and rain). Recently, the Goddard 3ICE schemes were modified to reduce over-estimated and unrealistic amounts of cloud water and graupel in the stratiform region

[2] The above Goddard microphysical scheme has been implemented into the MM5 and ARPS.

(Tao *et al.* 2003a; Lang *et al.* 2007). Various assumptions associated with the saturation technique were also revisited and examined (Tao *et al.* 2003a). Table 2 shows the list of microphysical processes that parameterize the transfer between water vapor, cloud water, rain, cloud ice, snow and graupel/hail in Goddard scheme implemented into WRF. The formula in each process can be found in Lin *et al.* (1983), Rutledge and Hobbs (1984), Tao and Simpson (1993), Tao *et al.* (2003a), and Lang *et al.* (2007). A Spectral Bin Microphysical (SBM) scheme is recently implemented into WRF V3.1.

	Cloud Water (QC)	**Rain (QR)**	**Cloud Ice (QI)**	**Snow (QS)**	**Graupel/Hail (QH)**
Condensation	CND				
Evaporation	*DD*	*ERN*			
Auto-conversion	*-PRAUT*	+PRAUT			
Accretion	*-PRACW*	+PRACW			
Deposition DEPOSITION OF QS DEPOSITION OF QG			PIDEP PINT DEP	PSDEP	
Sublimation			*-DD1*	*-PSSUB*	
Melting	PIMLT	PSMLT PGMLT	-PIMLT	*-PSMLT*	*-PGMLT*
AUTOCONVERSION OF QI TO QS			*-PSAUT*	PSAUT	
ACCRETION OF QI TO QS			*-PSACI*	PSACI	
ACCRETION OF QC BY QS (RIMING) (QSACW FOR PSMLT)	*-PSACW* *-QSACW*	QSACW		PSACW	
ACCRETION OF QI BY QR			*-PRACI*	del3* PRACI	(1-del3)* PRACI
ACCRETION OF QR OR QH BY QI		*-PIACR*		del3* PIACR	(1-del3)* PIACR
BERGERON PROCESSES FOR QS	*-PSFW*			PSFW	
BERGERON PROCESSES FOR QS			*-PSFI*	PSFI	
ACCRETION OF QS BY QH (DGACS,WGACS: DRY AND WET)				*-PGACS* *-DGACS* *-WGACS*	PGACS DGACS WGACS
ACCRETION OF QC BY QH (QGACW FOR PGMLT)	*-DGACW* *-QGACW*				DGACW QGACW
ACCRETION OF QI BY QH (WGACI FOR WET GROWTH)			*-DGACI* *-WGACI*		DGACI WGACI
ACCRETION OF QR TO QH (QGACR FOR PGMLT)		*-DGACR* *-(1-del)* WGACR* *-del* WGACR*			DGACR WGACR
WET GROWTH OF QH					
SHED PROCESS		QGACW		WGACR= PGWET- DGACW- WGACI- WGACS	QGACW
AUTOCONVERSION OF QS TO QH				*-PGAUT*	PGAUT
FREEZING		*-PGFR*			PGFR
ACCRETION OF QS BY QR				*-PRACS*	PRACS
ACCRETION OF QR BY QS (QSACR FOR PSMLT)		*-PSACR*		del2* PSACR	(1-del2)* PSACR
HOMOGENEOUS FREEZING OF QC TO QI (T < T00)	*-PIHOM*		PIHOM		
DEPOSITION GROWTH OF QC TO QI	*-PIDW*		PIDW		

Table 2 List of microphysical processes (abbreviation and brief description) that parameterize the transfer between water vapor, cloud water, rain, cloud ice, snow and graupel/hail in Goddard scheme implemented into WRF. Please note that the source term is regular font and sink term is italic font. The formula in each process can be found in Lin et al. (1983), Rutledge and Hobbs (1984), Tao and Simpson (1993), Tao et al. (2003a), and Lang et al. (2007). Del, del2 and del3 are 1 or 0 and depend on the value of the mixing ratio of cloud species (see Lin et al. 1983).

Note that the Goddard 3ICE scheme has been used for the CWB-WRF operational scheme since April 2008. Co-PI, Ms. Chang has recently used the Goddard 3ICE scheme in WRF3.1 to conduct (1) *SoWMEX/TiMREX IOP cases (IOP5 and IOP8)*, (2) Typhoon Morakot 2009 and (3) real time for 2009. In addition, the Goddard improved microphysics and radiation scheme (see descriptions in section 3) were recently provided to the Co-PI, Mei-Yu Chang for testing in CWB's WRF3.1.1.

3. Results

3.1 Radiation

PI was asked by CWB to examine the WRF RRTM scheme and its associated cloud radiative properties. It is found that the threshold for determining the effect of cloud on radiative heating/cooling is large in RRTM compared to Goddard radiation scheme. In addition, one of the precipitating clouds (graupel or hail) is not considered in the RRTM (although the effect of large precipitating particles is not significant compared to small non-precipitating particles). The preliminary results suggested that the impact of changing the threshold is not significant for short-term model integration (i.e., 24 h forecast). However, it could have impact on radiation budget and for long-term model integration (i.e., monthly regional climate simulation).

(a) Radiative Transfer

The parameterizations developed by Chou and Suarez (1999) for shortwave radiation and by Chou *et al.* (1995), Chou and Kouvaris (1991), Chou *et al.* (1999), and Kratz *et al.* (1998) for longwave radiation have been implemented into the WRF model. The solar radiation scheme includes absorption due to water vapor, CO_2, O_3, and O_2. Interactions among the gaseous absorption and scattering by clouds, aerosols, molecules (Rayleigh scattering), and the surface are fully taken into account. Fluxes are integrated virtually over the entire spectrum, from 0.175 μm to 10 μm. The spectrum is divided into seven bands in the ultraviolet (UV) region (0.175-0.4 μm), one band in the photosynthetically active radiation (PAR) region (0.4-0.7 μm), and three bands in the near infrared region (0.7-0.10 μm). In the UV and PAR region, a single O_3 absorption coefficient and a Rayleigh scattering coefficient are used for each of the eight bands. The O_3 absorption coefficient is taken from the spectral values given in WMO (1985). In the infrared, the k-distribution method is applied to compute the absorption of solar radiation. Ten k-distribution functions (equivalently, ten k values) are used in each of the three bands. The one-parameter scaling is used to compute the absorption coefficient in individual layers where temperature and pressure vary with height. The absorption due to O_2 is derived from a simple function, and the absorption due to CO_2 is derived from pre-computed tables. Reflection and transmission of a cloud and aerosol-laden layer are computed using the d-Eddington approximation. Fluxes for a composite of layers are then computed using the two-stream adding approximation.

In computing thermal infrared fluxes, the spectrum is divided into nine bands. As in the solar spectral region, the k-distribution method with temperature and pressure scaling is used to compute the transmission function in the weak absorption bands of water vapor and minor trace gases (N_2O, CH_4, CFC's). Six values of k are used for water vapor absorption, and only a few values of k are used for the minor trace gases. For the strong absorption bands of water vapor, the 15-μm CO_2 band, and the 9.6-μm O_3 band, the cooling is strong in the upper stratosphere. The use of the k-distribution method with the one-parameter temperature and pressure scaling induces a large error in the cooling rate above the 10-mb level. Instead, a look-up table method is used to compute the transmission function

in the strong absorption bands, which computes accurately the cooling rate from the surface to the 0.01-mb level.

(b) Cloud Optical Properties

The use of a fully explicit microphysics scheme (liquid and ice) and a fine horizontal resolution (5 km or less) can simulate realistic cloud optical properties, which are crucial for determining the radiation budgets. With high spatial resolution, each atmospheric layer is considered either completely cloudy (overcast) or clear. No partial cloudiness is assumed. For detailed discussion on cloud optical properties can be found in Tao *et a*l. (2003).

Predicted radiative cooling and heating rates at cloud-top from both methods are on the order of 30 to 50 ^{O}K/day, which is in good agreement with Ackerman *et al*. (1988) and Stephens (1978). Sensitivity tests have been performed to examine the impact of various cloud optical property calculations on rainfall. The results show that the impact of the various cloud optical property calculations is greater in tropical cases, 3-5% compared to just 1-2% for midlatitude cases.

3.2 Improved microphysical scheme

(a) An improved rain evaporation process

By comparing the bulk and spectral bin microphysics, it was found that the evaporation of rain in the bulk scheme is usually too large. An empirical correction factor—$r(qr) = 0.11q^{-1.27}r + 0.98$, where q_r is the rain mixing ratio (g kg^{-1})—is developed to correct the overestimation of rain evaporation in the bulk scheme (Li *et al*. 2009). Applying $r(q_r)$ in the bulk scheme produces spatial and temporal variation modes similar to those in sensitivity tests using the mean evaporation reduction factor. However, using $r(q_r)$ consistently results in a larger stratiform area. Similarly, it is possible to modify the ice phase microphysics in the bulk simulation using the bin scheme. However, ice phase microphysics has many uncertainties, including ice initiation and multiplication and the density, shape, and terminal fall velocity of various ice species and their interactions with one another. Many fundamental processes in ice microphysics are still being actively researched. Planned future study includes validating the ice microphysics in the bin scheme using both in situ and remote observations. After gaining confidence in the bin simulation, it will then be used to improve bulk microphysical schemes.

(b) An improved microphysical scheme to reduce 40dBz at high altitude

It is needed to continue examining and improving the performance of the WRF's bulk microphysics schemes. For example, there is a well-known bias in bulk schemes, which tend to generate excessively large reflectivity values (e.g., 40 dBZ) aloft due to graupel (e.g., Lang *et al*. 2007; Li *et al*. 2009). This bias is also related to a bias in excessive simulated ice scattering. The performance of the GCE bulk microphysics scheme was improved by reducing the bias in over penetrating 40-dBZ echoes at higher altitudes (Fig. 1), which is due mainly to excessively large amounts and/or sizes of graupel particles at those altitudes. This also improved the overall model reflectivity probability distribution (i.e., CFADs). These improvements were achieved by systematically evaluating and improving individual ice processes in the bulk scheme such as: (1) accounting for relative humidity and mean cloud ice mass in the Bergeron process for snow, (2) adding a simple Hallett-Mossop rime splintering parameterization, (3) replacing the Fletcher curve, which determines the number of active ice nuclei as a function of temperature, with the Meyers *et al*. (1992) curve, which determines the active ice nuclei as a function of ice supersaturation, in the cloud ice nucleation, depositional growth

and Bergeron growth parameterizations, (4) relaxing the saturation scheme to allow for ice supersaturation, (5) adding two additional parameterizations for contact nucleation and immersion freezing, (6) including cloud ice fall speeds, (7) allowing graupel and snow to sublimate (the original R&H scheme only allows graupel and snow deposition but not sublimation, and (8) mapping the snow and graupel intercepts (effectively the mean snow and graupel particle diameters) as functions of temperature and mass.

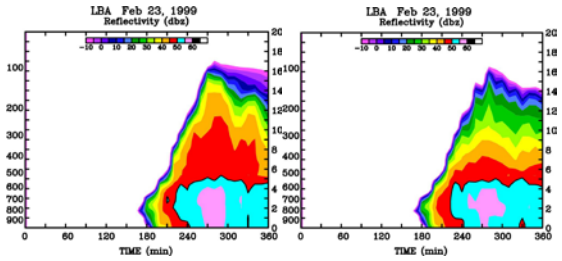

Fig. 1 *Time-height cross sections of maximum radar reflectivity obtained from 3D simulations of the 23 February 1999 easterly regime event observed during TRMM LBA (Large Scale Biosphere-Atmosphere Experiment in Amazonia) using the original Rutledge and Hobbs (1984) based bulk microphysics formulation (left panel) and an improved version (right panel). Climatologically, 40-dBZ penetrations above 10 km are rare even over land (Zipser et al. 2006; Liu et al. 2008). Ground-based radar data for this case indicated 40-dBZ echoes reached to approximately 8 km.*

3.3 Convective and stratiform separation method

In the CRM model simulation, the simulated cloud characteristics can be divided into their convective and stratiform components (Tao *et al.* 1991, 1993b; Lang *et al.* 2003). In short, convective regions include those with large vertical velocities (exceeding 3-5 m s^{-1}) and/or large surface precipitation rates. The stratiform region is separated into regions with and without surface rainfall. The separation method was implemented into WRF and was tested in offline for the early (more convective), and mature stage of the convective system. The convective and stratiform separation software would provide a statistical evaluation of cloud and precipitation processes in WRF.

3.4 Perform high-resolution model simulations associated with deep convective events

To examine the generality and applicability of the microphysical schemes, several different types of precipitation systems were selected to test the performance of the Goddard microphysical scheme with its different options (i.e., 2ICE and both 3ICE versions).

(a) Conduct high-resolution model simulations

We have conducted sensitivity tests in terms of model grid mesh for a heavy precipitation event. The preliminary result also indicates that the 3ICE with hail option simulated maximum rainfall is larger and in better agreement with observation compared with 3ICE with graupel option (Table 3). The comparison with simulated radar reflectivity (pattern and intensity) also indicated that the 1 km grid resolution simulation is in better agreement with observation than the 6 km grid simulation (not shown).

Grid resolution	3ice scheme	Maximum Rainfall
1 km	Cloud ice, snow and hail	307.7 mm
1 km	Cloud ice, snow and graupel	236.5 mm
2 km	Cloud ice, snow and graupel	178.4 mm
6 km	Cloud ice, snow and graupel	168.1 mm
Observation		294.0 mm

Table 3 *The maximum rainfall simulated by model with different grid spacing (1, 2 or 6 km) and different Goddard microphysical options (hail or graupel). Observed maximum rainfall is also shown for comparison.*

We will continue performing the sensitivity tests to investigate the impact of the horizontal grid sizes and numbers of vertical layers on the modeled predicted strength and evolution of rainfall. Numerical experiments will be performed for selected severe weather events over the Taiwan area (see next section). In addition, contoured frequency with altitude diagrams (CFADs) (Yuter and Houze 1995) will be constructed to examine the frequency distributions of various fields as a function of height.

(b) Typhoon Morakot (2009) case

Typhoon Morakot struck Taiwan on the night of Friday August 7th, 2009 as a category 2 storm with sustained winds of 85 knots (92 mph). Although the center made landfall in Hualien county along the central east coast of Taiwan and passed over the central northern part of the island, it was southern Taiwan that received the worst effects of the storm where locally as much as 2000 mm of rain were reported, resulting in the worst flooding there in 50 years. Figure 3 shows the observed surface rainfall distribution.

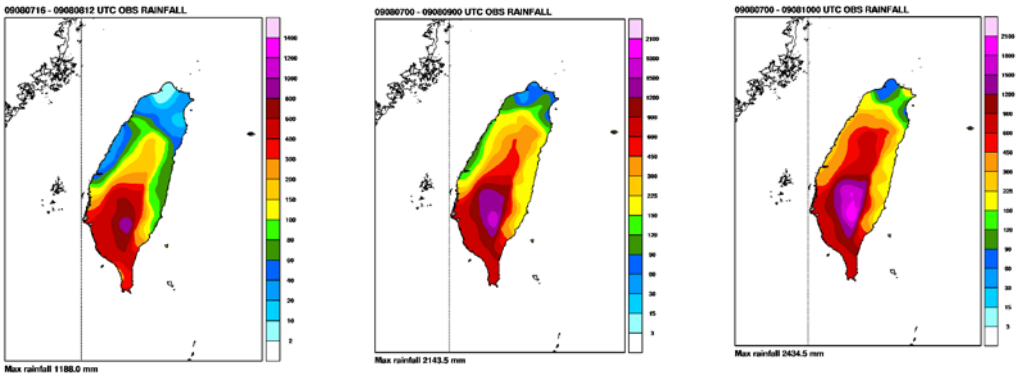

Fig. 3 *Twenty (20)-h ((from 00 Z August 8 to 20 Z August 8, left panel), 48-h (from 08 Z August 7 to 08 Z August 9, middle panel) and 72-h (from 08 Z August 7 to 08 Z August 10, right panel) accumulated observed surface rainfall (mm). Note that the significant rainfall continued in the same locations (S. Taiwan) over the 72-h period.*

Morakot began as a tropical depression on the morning of the 4th of August (local time) in the central Philippine Sea about midway between the Northern Mariana Islands and Taiwan. The system strengthened into a tropical storm later on the 4th and became a typhoon on the morning of the 5th as is tracked due westward toward Taiwan. Morakot maintained category 1 (in intensity) on the 6th with sustained winds estimated at 80 knots (~92 mph) by the Joint Typhoon Warning Center. The storm briefly reached category 2 (in intensity) with sustained winds of 85 knots (~98 mph) as it neared the coast of Taiwan on the 7th. Over the next two days, there are extremely heavy amounts of rain over the southern half of Taiwan, which is on the southern side of the storm track. Nearly the entire southern half of the island has in excess of 1000 mm of rain. Within that are areas in excess of 1000 mm along the western slopes of the central mountain range (see Fig. 3). The result of the enormous amount of rain has been massive flooding and devastating mudslides. More than 600 people are confirmed dead (including hundreds of people in Shiao Lin, which was destroyed by a large mudslide). Shiao Lin is located on the western side of the central mountain range in south central Taiwan. On 9 August 2009, the center of Morakot had already passed over Taiwan and was just about to make landfall on the east coast of Mainland China. However, a large rain band of light to moderate rain

with embedded areas of heavy rain oriented southwest to northeast still over southern Taiwan. This feature reveals the reason for the heavy amounts of rain over the southern portion of the island (Fig. 3): persistent southwesterly flow associated with Morakot and it's circulation was able to draw up copious amounts of moisture from the South China Sea into southern Taiwan where it was able to interact with the steep topography.

The WRF V3.1 with improved microphysics (described in Section 3.2) is used to simulate this typhoon case. Fig. 4 shows the WRF domain, with 18, 6 and 2 km with corresponding numbers of grid points 391x322x61, 475x427x61, 538x439x61, respectively. Time steps of 60, 20 and 6.667 seconds are used in these nested grids, respectively. The Grell-Devenyi (2002) cumulus parameterization scheme was used for the outer grid (18 km) only. For the inner two domains (6 and 2 km), the Grell-Devenyi parameterization scheme was turned off. The planetary boundary layer parameterization employed the Mellor-Yamada-Janjic (Mellor and Yamada 1992) turbulence closure model. The surface heat and moisture fluxes (from both ocean and land) were computed from similarity theory (Monin and Obukhov 1954). The land surface model is based on Chen and Dudhia (2001). It is a 4-layer soil temperature and moisture model with canopy moisture and snow cover prediction. The Goddard broadband two-stream (upward and downward fluxes) approach was used for the shortwave and longwave radiative flux calculations (Chou and Suarez 1999). The model was initialized from NOAA/NCEP/GFS global analyses (1.0^{o} by 1.0^{o}). Time-varying lateral boundary conditions were provided at 6-h intervals.

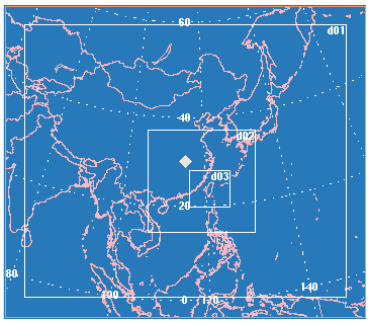

Fig. 4 WRF Inter-nesting model configuration used for Typhoon Moratok case. Horizontal resolutions for domains are 18, 6 and 2 km, respectively.

Figures 5 and 6 show the WRF-simulated rainfall from four different options (3ICE-hail with reducing rain evaporation, original 3ICE-graupel, improved 3ICE-graupel and Warm Rain only) in the Goddard microphysical scheme. Generally speaking, WRF produced the right distribution of precipitation for this typhoon case despite using different Goddard microphysical options. For example, in all of the runs the main precipitation event is elongated in the southwest-northeast direction and organizes into a convective line near the Southern Taiwan as observed (Fig. 3). All of the schemes resulted in simulations wherein the main area of precipitation continued over Southern Taiwan over the 72-h period. This feature also generally agrees with observations (Fig. 3). The results (with high resolution visualization) also show that a persistent (over 48 h) southwesterly flow associated with Morakot and its circulation was able to draw up copious amounts of moisture from the South China Sea into southern Taiwan where it was able to interact with the steep topography in all four microphysical options. This result suggests that the major rainfall distribution is determined by the large-scale circulation pattern (Typhoon induced circulation) for this Morakot case. The interaction between the terrain and moisture flux are the key processes to cause floods /landslides for this case. However, less rainfall is simulated in warm rain only option compared to those with ice processes (see Table 4). This clearly indicated that ice processes are important for producing significant rainfall for this typhoon case. All ice schemes also produced more than 2000 mm accumulated rainfall over south Taiwan. The improved 3ICE-graupel option simulated maximum rainfall amount is in better

agreement with observation than the other two ice options (Table 4). However, the improved 3ICE-graupel might produce more rainfall over east-northern Taiwan in the early stages of model simulation (Fig. 5).

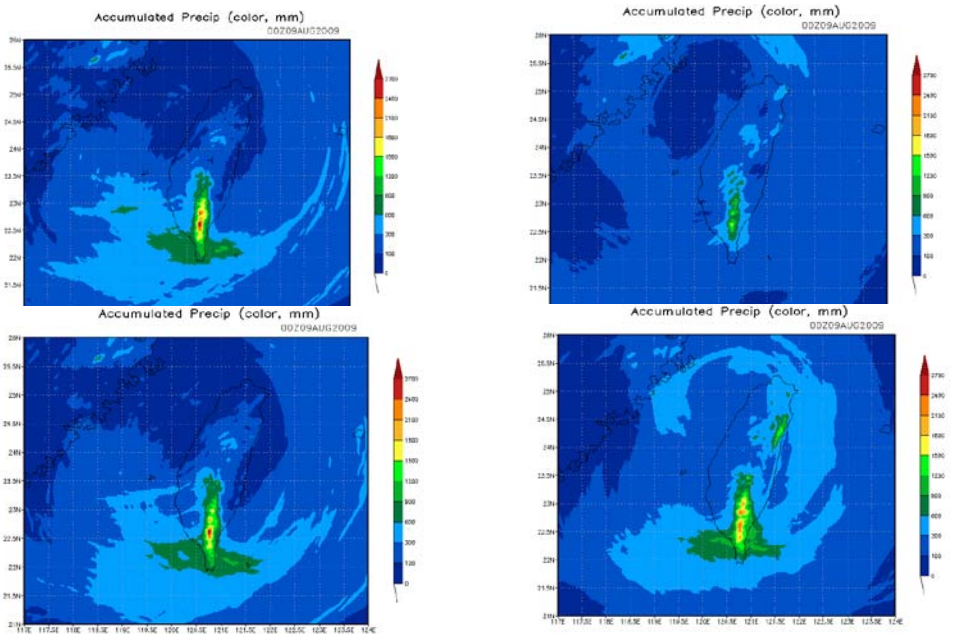

Fig. 5 WRF simulated accumulated-surface rainfall (mm) from 08Z 8/7 to 08Z 8/9, 2009 using Goddard 3ICE microphysical schemes. Top two panels are 3ICE-hail with reduced rain evaporation (left) and one with warm rain only (right), respectively. The bottom panels are with original 3ICE-graupel (left) and with improved 3ICE-graupel (right), respectively.

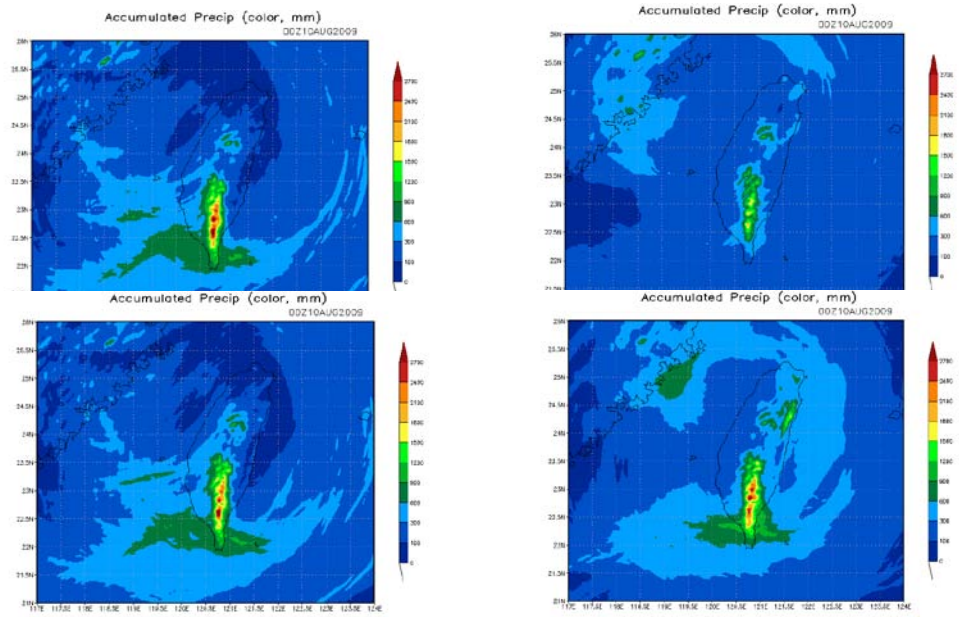

Fig. 6 Same as Fig. 5 except for 72-h WRF simulated accumulated-surface rainfall (mm).

Microphysical schemes	48 – hours Maximum Rainfall (mm)	72-hours Maximum Rainfall
3ICE-Hail with reduced Evaporation	**2867**	**3307**
3ICE-Graupel	**2856**	**3345**
3ICE – Graupel Improved	**2396**	**2942**
Warm Rain Only	**1589**	**2000**
Observation	**2134**	**2434**

Table 4 The maximum rainfall simulated by model with different Goddard microphysical options (include improved as described in Section 3.2). Observed maximum rainfall is also shown for comparison.

(c) SoWMEX/TiMREX 2008

Several major precipitation events (i.e., observed during the SoWMEX/TiMREX 2008) that developed over the Taiwan region were selected for examining the performance of the cloud microphysics parameterization on precipitation processes and its predicted rainfall. The selection of these cases will be consulted with CWB operational forecasters and researchers. For example, Co-PI., Ms. Chang, has conducted case studies (IOP6 and IOP8 and see Table 5) observed during SoWMEX/TiMREX in 2008. Sensitivity tests are performed to examine the impact of microphysics (2ICE, 3ICE-graupel, 3ICE-hail), horizontal resolution (5 and 2.5 km), and vertical layers (45 vs 61 layers) on simulated rainfall amount and patterns. Generally, the 3ICE-hail simulates in better agreement with observed radar reflectivity than using either 2ICE or 3ICE-graupel. For example, the simulated rainfall is mainly over the southern region of Taiwan as seen in observation (Fig. 7). In addition, the results suggested that the 5-km grid simulated stronger (or more intense) rainfall than those of 2-km grid (Fig. 8). In addition, the more vertical layers simulated more intense rainfall for the 2-km grid simulation. The 2-km grid with 61-vertical layers seems to simulate better rainfall patterns.

PI and co-PI plan to continue conducting detailed analyses and comparisons with observations (Typhoon Morakot and SoWMEX/TiMREX cases). We will evaluate model forecasts with ground-based observations (i.e., radar, rain gauge) and satellite data. Model estimates of radar reflectivity will be produced from the simulated precipitation using the characteristics of the microphysics properties (i.e., hydrometeor type, size distribution). Actual radar reflectivity (in convective or heavy rainfall region and stratiform or light rainfall region) can then be interpolated to WRF grid to facilitate comparisons similar to the QPF evaluations. We will use the contoured frequency with altitude diagrams (CFADs)[3] to examine the frequency distributions of various fields as a function of height. The validation of model microphysics needs to work with CWB operational group.

IOP#	Date	Science objectives
1 (a & b)	06Z May 19 to 00Z May 22	Frontal circulation Upstream environment for orographic convection
2	06Z May 27 to 21Z May 29	Southwest flow interacting with the terrain Upstream condition for mountain convection - Lee side vortex/shear zone
3	21Z May 29 to 12Z May 31	Island effects on SW (LLJ) and the Mei- Yu front Upstream condition forheavy precipitation
4	21Z June 1 to15Z June 3	Mesoscale convective systems Shallow surface front - Mesoscale convective vortex
5	18Z June 3 to 12Z June 4	Mesoscale convective systems Quasi-stationary front - Mesoscale convective vortex
6	**18Z June 4 to 12Z June 6**	**Mesoscale convective systems** **Quasi-stationary front - Mesoscale convective vortex**
7	00Z June 12 to 12Z June 13	Convection initiation - Orographic convection

[3] This CFAD program including the subroutine for computing radar reflectivity has been provided to Co-PI. Ms. Mei-Yu Chang in 2008.

8	**00Z June 14 to 12Z June 17**	**Southwesterly flow interacting with the terrain Upstream condition for mountain convection, low level jet Mesoscale convective systems - Mesoscale convective vortex**
9	06Z June 23 to 12Z 26 June	Typhoon Fengseng track uncertainty Typhoon induced southwesterly flow and related heavy rain systems

Table 5 The summary of SoWMEX/TiMREX IOP cases (kindly provided by Dr. Pay-Liam Lin). Red indicated the cases (IOP6 and IOP8) have been conducted by Ms. Mei-Yu Chang

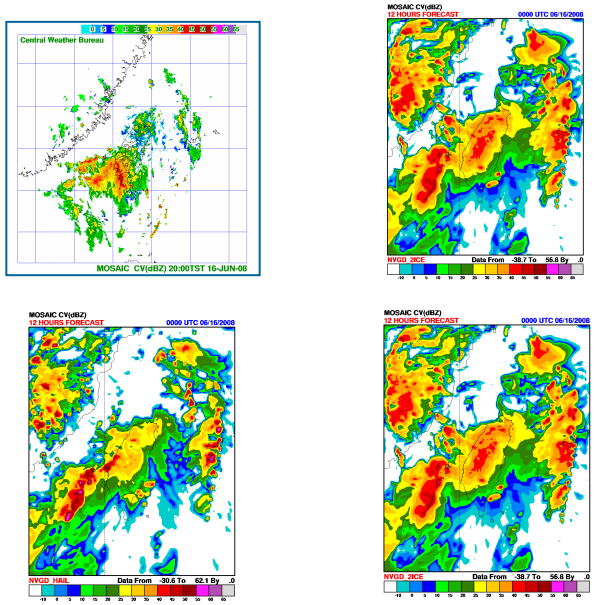

Fig. 7 CWB's WRF simulated surface rainfall (mm) at 20:00 Z (UTC) on June 6 2008 using Goddard 3ICE microphysical schemes. Top two panels are observed (left) and one with 2ICE scheme (right), respectively. The bottom panels are with 3ICE-hail (left) and with 3ICE-graupel (right), respectively. A 5-km grid is using for these sensitivity tests.

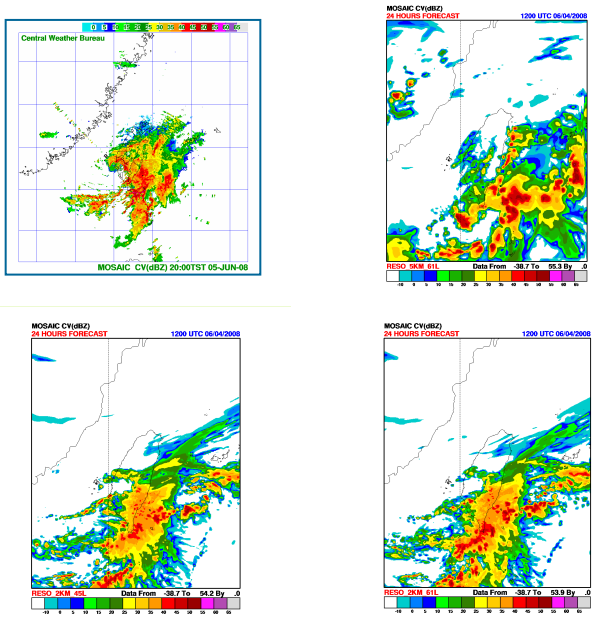

Fig. 8 CWB's WRF simulated surface rainfall (mm) at 20:00 Z (UTC) on June 4 2008 using Goddard 3ICE microphysical scheme. Top two panels are observed (left) and one with - km and 61-vertical layers

(right), respectively. The bottom panels are with - km and 45-vertical layer (left) and with 2-km and 63-vertical layer (right), respectively. The Goddard 3ICE-graupel is used for these sensitivity tests.

(d) Real time forecasts

The Goddard 3ICE schemes with Goddard radiation schemes have been provided to the Co-PI, Ms. Mei-Yu Chang for testing. Ms. Chang has recently conducted a real-time forecast for typhoon Morokot case to examine the performance of the Goddard 3Ice scheme. Sensitivity tests have been done on the impact of microphysics on precipitation processes with high-resolution 45 x 15 x 5 km with corresponding numbers of grid points 221x121x45, 181x193x45, 148x178x45, respectively. Time steps of 180, 90, and 30 seconds were used in these nested grids, respectively. The Kain-Fritsch cumulus parameterization scheme was used for the outer grid (45 and 15 km grid mesh) only. For the inner domain (5 km grid mesh), the parameterization scheme was turned off. The planetary boundary layer parameterization employed the YSU turbulence scheme. The surface heat and moisture fluxes (from both ocean and land) were computed from the similarity theory (Monin and Obukhov 1954). The land surface model is based on a thermal diffusion scheme that provides sensible and latent heat fluxes to the boundary layer scheme (Noah LSM)). The longwave scheme is based on Mlawer *et al.* (1997) and is a spectral-band scheme using the correlated-k method. For shortwave radiative transfer processes, the Goddard scheme is used. Three tests are conducted to examine the impact of initial and lateral boundary condition, and update cycle (Table 6). Both NCEP-GFS and CWF-GFS utilized the data assimilation. The model is integrated from 00 UTC August 6 to 12 UTC August 10, 2009.

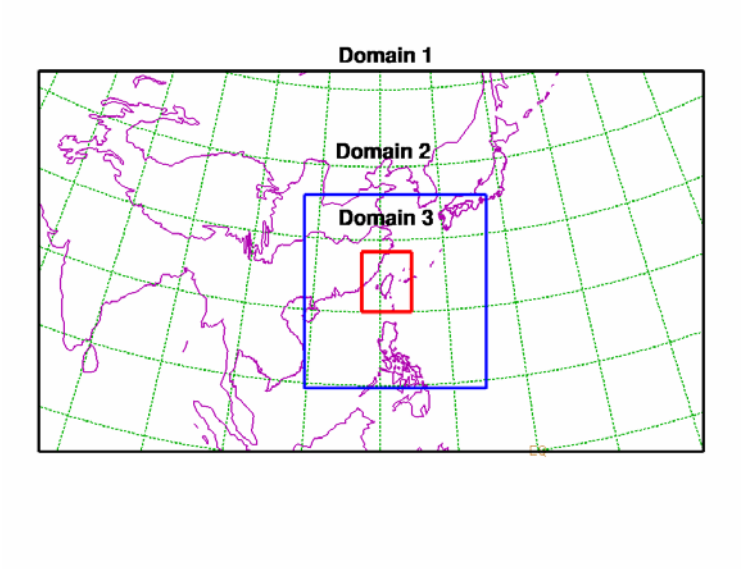

Fig. 9 Nesting configuration used for the Typhoon Morakot case. Horizontal resolutions for domains are 45, 15 and 5 km, respectively.

System	Initial and Boundary Condition	Update Cycle
WRF-M00	NCEP-GFS	Full-updated
WRF-M01	NCEP-GFS	Limited-updated
WRF-M02	CWB-GFS	Full-updated

Table 6 The initial and boundary conditions and update cycle used in the WRF forecast system.

Figure 10 shows the WRF predicted rainfall amount for Typhoon Morakot. The results suggested that less rainfall was simulated for the 15-km grid than that of the 5-km grid. The results also suggest that better rainfall was simulated with 24-h forecast than those of 48-h forecast. Both results show that NWP has better rainfall forecast ability with higher resolution and shorter integration.

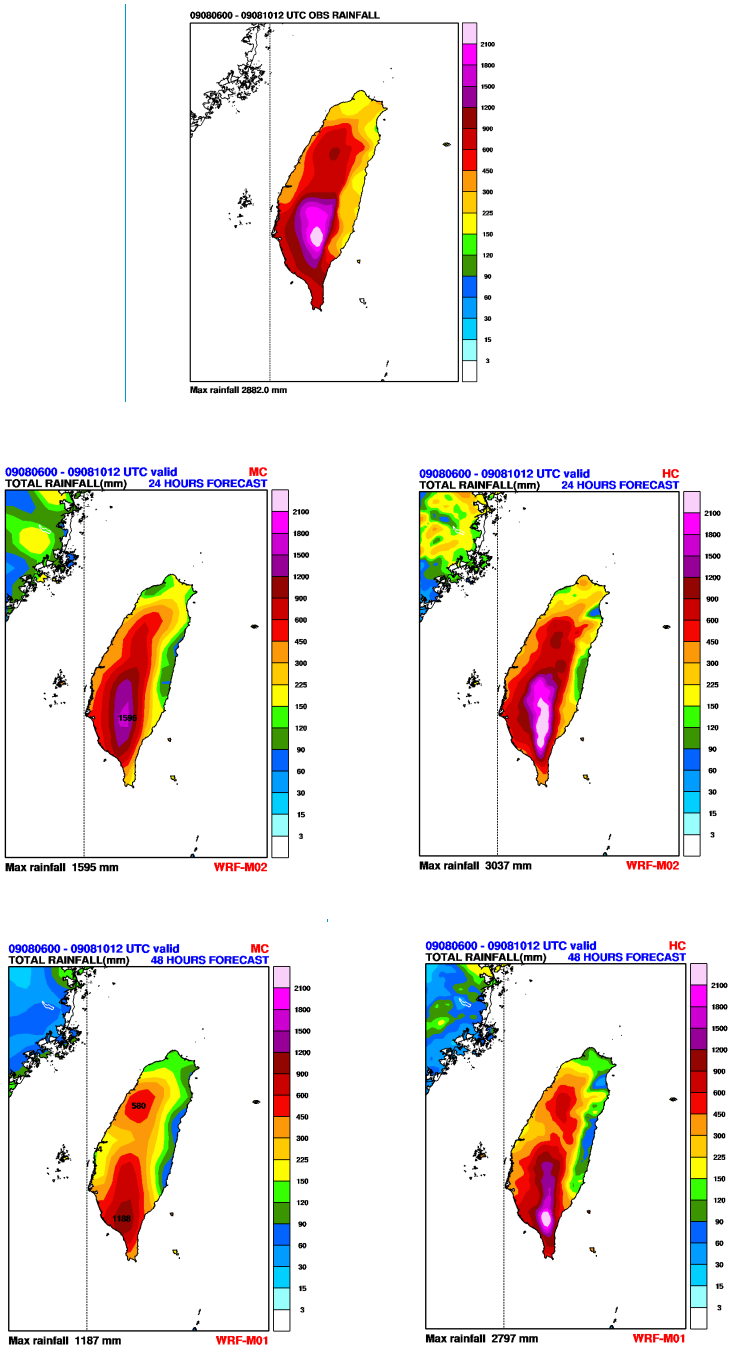

Fig. 10 CWB's WRF simulated accumulated surface rainfall (mm) from 06 UTZ August 8 to 12:00 UTZ August 10 2009 using Goddard 3ICE microphysical schemes. Top panel is observed, and the middle and bottom panel show the WRF simulated. The middle and bottom panels are 24-h and 48-h forecast, respectively. The left panel and right panels show the 15-km and 5-km grid simulated rainfall,

respectively.

Tables 7 and 8 show the statistics / scores (bias, maximum rainfall amount) from WRF forecasts. The results clearly show that the WRF simulations with 5-km grids have better rainfall forecasts than those with coarser resolutions (15 and 45 km grid mesh). For example, the 5-km domain simulated maximum rainfall ranges from 62 to 105% as observed. These maximum rainfalls are at least 30% to 70% better than those from 15-km and 45-km grid model, respectively. These results suggest that the higher model resolution could help improving the rainfall forecast. Also the results show that the WRF simulated rainfall has better bias (mean of all rainfall thresholds) with full updated cycle than the case with limited updated cycle. These runs with 15-km and 5-km grid models also have very good bias (> 0.80). In addition, the 12-h rainfall forecast is in very good agreement with observation. The 12-h forecast is also better than those with 24-h, 36-h and 48-h forecast.

	0-12 h	***12-24 h***	***24-36 h***	***36-48 h***
M00-45 km	12.60%	12.14%	10.17%	7.81%
M01-45 km	19.08%	15.79%	12.49%	12.77%
M02-45 km	12.39%	12.80%	10.27%	6.63%
	0-12 h	***12-24 h***	***24-36 h***	***36-48 h***
M00-15 km	47.29%	44.97%	55.14%	51.32%
M01-15 km	44.24%	34.98%	39.17%	41.19%
M02-15 km	47.05%	55.34%	47.99%	39.31%
	0-12 h	***12-24 h***	***24-36 h***	***36-48 h***
M00-5 km	74.50%	88.62%	98.92%	76.16%
M01-5 km	76.27%	68.63%	99.93%	97.05%
M02-5 km	78.59%	105.38%	80.05%	62.56%
Mean – 5km	76.45%	87.54%	92.97%	78.59%

Table 7 Model performance in maximum rainfall forecast in percentage represented by the ratio between forecast maximum rainfall and observed maximum rainfall.

	0-12 h	***12-24 h***	***24-36 h***	***36-48 h***	***Averaged***
M00-45 km	0.584	0.499	0.441	0.390	0.479
M01-45 km	0.674	0.594	0.548	0.506	0.581
M02-45 km	0.592	0.548	0.459	0.407	0.502
Averaged	0.616	0.574	0.482	0.434	0.520
	0-12 h	***12-24 h***	***24-36 h***	***36-48 h***	
M00-15 km	0.753	0.810	0.833	0.796	0.817
M01-15 km	0.829	0.678	0.766	0.676	0.736
M02-15 km	0.882	0.880	0.863	0.759	0.847
Averaged	0.821	0.783	0.837	0.744	0.800
	0-12 h	***12-24 h***	***24-36 h***	***36-48 h***	
M00-5 km	0.997	0.871	0.891	0.848	0.902
M01-5 km	0.909	0.766	0.831	0.749	0.814
M02-5 km	1.050	0.953	0.890	0.804	0.924
Averaged	0.985	0.863	0.871	0.800	0.880

Table 8 Model performance in bias including the mean of all rainfall thresholds.

We will continue improving the performance of the CWB WRF's bulk microphysics schemes and investigate the sensitivity of model resolution on precipitation processes and surface rainfall intensity.

4. CWB Visit

The PI, W.-K. Tao, has visited the CWB and worked with Ms. Chang the week of April 6 2009. He also presented a talk to CWB and its title is "*The impact of microphysics on hurricane and the impact of resolution on cloud development*". In this talk, he presented: (a) A review on previous modeling studies in terms of sensitivity tests of microphysics on the intensity and track of hurricanes/typhoons, (b) The impact of resolution on rainfall intensity and patterns on a heavy precipitation event in Taiwan, and (c) The impact of horizontal resolution on microphysical processes.

During the visit to CWB, Tao has provided the new improvement of microphysical processes to the Co-I. Ms. Mei-Yu Chang of CWB. Tao and Ms. Chang will be implementing these improvements into CWB's WRF (V3.1) this summer. He also discussed the radiative processes with Co-I., and other CWB scientists.

5. Reference (not complete, will provide as requested)

Colle B. A., and Y. Zeng, 2004b: Bulk microphysical sensitivities and pathways within the MM5 for orographic precipitation. Part II: Impact of different bulk schemes, barrier width, and freezing level. *Mon. Wea. Rev.*, **132**, 2802–2815

Cotton, W. R., M. A. Stephens, T. Nehrkorn and G. J. Tripoli, 1982: The Colorado State University three-dimensional cloud-mesoscale model-1982. Part II: An ice-phase parameterization. *J. Rech. Atmos.,* **16**, 295-320.

Cotton, W. R., G. J. Tripoli, R. Rauber and E. Mulvihill, 1986: Numerical simulation of the effects of varying ice crystal nucleation rates and aggregation processes on orographic snowfall. *J. Climate Appl. Meteor*., **25**, 1658-1680.

Ferrier, B. S., 1994: A double-moment multiple-phase four-class bulk ice scheme. Part I: Description. *J. Atmos Sc.i*, **51**, 249-280.

Ferrier, B.S., W.-K. Tao and J. Simpson,1995: A double-moment multiple-phase four-class bulk ice scheme. Part II: Simulations of convective storms in different large-scale environments and comparisons with other bulk parameterizations. *J. Atmos Sci.*, **52**, 1001-1033.

Fovell, R. G., and Y. Ogura, 1988: Numerical simulation of a midlatitude squall line in two-dimensions. *J. Atmos. Sci.*, **45**, 3846-3879.

Fritsch, J. M., and R. E. Carbone, 2002: Research and development to improve quantitative precipitation forecasts in the warm season: A synopsis of the March 2002 USWRP Workshop and statement of priority recommendations. *Technical report to UEWRP Science Committee*,134pp.

Fu, Q., S. K. Krueger, and K.-N. Liou, 1995: Interaction of radiation and convection in simulated tropical cloud clusters. *J. Atmos. Sci.*, **52**, 1310-1328.

Gallus, W. A., Jr., 1999: Eta simulations of three extreme precipitation events: Sensitivity to resolution and convective parameterization. *Wea. Forecasting*, **14**, 405-426.

Hong, S.-Y., and J.-O. J. Lim, 2006: The WRF Single-Moment 6-Class Microphysics Scheme (WSM6). *J. Korean Meteor. Soc*., **42**, 2, 129-151.

Koenig, L. R., and F. W. Murray 1976: Ice-bearing cumulus cloud evolution: Numerical simulation and general comparison against observations. *J. Appl. Meteor*., **15**, 747-762.

Krueger, S. K., Q. Fu, K. N. Liou, and H.-N. Chin, 1995: Improvments of an ice-phase microphysics parameterization for use in numerical simulations of tropical convection. *J. Appl. Meteor.*, **34,** 281–287.

Lang, S., W.-K. Tao, R. Cifelli, W. Olson, J. Halverson, S. Rutledge, and J. Simpson, 2007: Improving simulations of convective system from TRMM LBA: Easterly and Westerly regimes. *J. Atmos. Sci.*, **64**, 1141-1164.

Lin, Y.-L., R. D. Farley and H. D. Orville, 1983: Bulk parameterization of the snow field in a cloud model. *J. Clim. Appl. Meteor.*, **22**, 1065-1092.

Liu, Y., D.-L. Zhang, and M. K. Yau, 1997: A multiscale numerical study of Hurricane Andrew (1992). Part I: An explicit simulation. *Mon. Wea. Rev.*, **125**, 3073-3093.

Lord, S. J., H. E. Willoughby and J. M. Piotrowicz, 1984: Role of a parameterized ice-phase microphysics in an axisymmetric, non-hydrostatic tropical cyclone model. *J. Atmos. Sci.*, **41**, 2836-2848.

McCumber, M., W.-K. Tao, J. Simpson, R. Penc, and S.-T. Soong, 1991: Comparison of ice-phase microphysical parameterization schemes using numerical simulations of tropical convection. *J. Appl. Meteor*., **30**, 985-1004.

Molinari, J., and M. Dudek, 1992: Parameterization of convective precipitation in mesoscale numerical models: A critical review. *Mon. Wea. Rev.*, **120**, 326-344.

Nicholls, M. E., 1987: A comparison of the results of a two-dimensional numerical simulation of a tropical squall line with observations. *Mon. Wea. Rev.*, **115,** 3055–3077.

Orville, H. D., and F. K. Kopp 1977: Numerical simulation of the life history of a hailstorm. *J. Atmos. Sci*., **34**, 1596-1618.

Rogers, R. F., and J. M. Fritsch, 1996: A general framework for convective trigger function. *Mon. Wea. Rev*., **124**, 2438-2452.

Rutledge, S.A., and P.V. Hobbs, 1983: The mesoscale and microscale structure and organization of clouds and precipitation in mid-latitude clouds. Part VIII: A model for the "seeder-feeder" process in warm-frontal rainbands. *J. Atmos. Sci*., **40**, 1185-1206.

Rutledge, S.A., and P.V. Hobbs, 1984: The mesoscale and microscale structure and organization of clouds and precipitation in mid-latitude clouds. Part XII: A diagnostic modeling study of precipitation development in narrow cold frontal rainbands. *J. Atmos. Sci.*, **41**, 2949-2972.

Soong, S.-T., and Y. Ogura, 1973: A comparison between axisymmetric and slab-symmetric cumulus cloud models. *J. Atmos. Sci.*, **30**, 879-893.

Tao, W.-K., and S.-T. Soong, 1986: A study of the response of deep tropical clouds to mesoscale processes: Three-dimensional numerical experiments. *J. Atmos. Sci.*, **43**, 2653-2676.

Tao, W.-K., J. Simpson, and S.-T. Soong, 1987: Statistical properties of a cloud ensemble: A numerical study. *J. Atmos. Sci.*, **44**, 3175-3187.

Tao, W.-K., and J. Simpson, 1989: Modeling study of a tropical squall-type convective line. *J. Atmos. Sci.*, **46**, 177-202.

Tao, W.-K., and J. Simpson, 1993: The Goddard Cumulus Ensemble Model. Part I: Model description. *Terrestrial, Atmospheric and Oceanic Sciences,* **4**, 19-54.

Tao, W.-K., J. Scala, B. Ferrier and J. Simpson, 1995: The effects of melting processes on the development of a tropical and a midlatitude squall line, *J. Atmos. Sci.*, **52**, 1934-1948.

Tao, W.-K., 2003: Goddard Cumulus Ensemble (GCE) model: Application for understanding precipitation processes, *AMS Meteorological Monographs - Cloud Systems, Hurricanes and TRMM*, 107-138.

Tao, W.-K., J. Simpson, D. Baker, S. Braun, M.-D. Chou, B. Ferrier, D. Johnson, A. Khain, S. Lang, B. Lynn, C.-L. Shie, D. Starr, C.-H. Sui, Y. Wang and P. Wetzel, 2003a: Microphysics, Radiation and Surface Processes in a Non-hydrostatic Model, *Meteorology and Atmospheric Physics*, **82**, 97-137.

Tao, W.-K., D. Starr, A. Hou, P. Newman, and Y. Sud, 2003b: Summary of cumulus parameterization workshop, *Bull. Amer. Meteor. Soc.*, **84**, 1055-1062.

Tao, W.-K., C.-L. Shie, D. Johnson, R. Johnson, S. Braun, J. Simpson, and P. E. Ciesielski, 2003c*:* Convective Systems over South China Sea: Cloud-Resolving Model Simulations *J. Atmos. Sci.*, **60**, 2929-2956.

Thompson, G., R. M. Rasmussen, and K. Manning, 2004: Explicit forecasts of winter precipitation using an improved bulk microphysics scheme. Part I: Description and sensitivity analysis, *Mon. Wea., Rev.*, **132**, 519-542.

Wang, W., and N. L. Seaman, 1997: A comparison study of convective parameterization schemes in a mesoscale model. *Mon. Wea. Rev*., **125**, 252-278.

Weisman, M. L., W. C. Skamarock and J. B. Klemp, 1997: The resolution dependence of explicitly modeled convective systems. *Mon. Wea. Rev*., **125**, 527-548.

Wu X., W. D. Hall, W. W. Grabowski, M. W. Moncrieff, W. D. Collins, and J. T. Kiehl, 1999: Long-term behavior of cloud systems in TOGA COARE and their interactions with radiative and surface processes. Part II: Effects of ice microphysics on cloud-radiation interaction. *J. Atmos. Sci.*, **56**, 3177–3195.

Yang, M.-J., and Q.-C. Tung, 2003: Evaluation of rainfall forecasts over Taiwan by four cumulus parameterization schemes. *J. Meteor. Soc. Japan*, **81**, 1163-1183.

Yoshizaki, M., 1986: Numerical simulations of tropical squall-line clusters: Two-dimensional model. *J. Meteor. Soc. Japan*, **64,** 469–491.

Yuter, S. and R. A. Houze Jr., 1995: Measurements of Raindrop Size Distributions over the Pacific Warm Pool and Implications for Z-R Relations, *J. Appl. Meteor*., 36, 847-867.

Zhang, D.-L., 1989: The effect of parameterized ice microphysics on the simulation of vortex circulation with a mesoscale hydroststic model. *Tellus*, **41A,** 132-147.

Zhang, D.-L., and X. Wang, 2004: Dependence of hurricane intensity and structures on vertical resolution and time step size. *Adv. Atmos. Sci*., 5, 711-725.

Zhu, T., and D.-L. Zhang, 2004: Numerical simulation of Hurricane Bonnie (1998). Part II: Sensitivity to varying cloud microphysical processes. *J. Atmos. Sci.*, **63**, 109-126.